University of Kentucky
UKnowledge

Toxicology and Cancer Biology Faculty Publications | Toxicology and Cancer Biology

9-15-2017

Loss of Fructose-1,6-Bisphosphatase Induces Glycolysis and Promotes Apoptosis Resistance of Cancer Stem-Like Cells: An Important Role in Hexavalent Chromium-Induced Carcinogenesis

Jin Dai
University of Kentucky, jindai@uky.edu

Yanli Ji
University of Kentucky

Wei Wang
University of Kentucky

Donghern Kim
University of Kentucky, donghern.kim@uky.edu

Leonard Yenwong Fai
University of Kentucky, leonardfai@uky.edu
Follow this and additional works at: https://uknowledge.uky.edu/toxicology_facpub

Part of the Cancer Biology Commons, Medical Toxicology Commons, and the Pharmacy and Pharmaceutical Sciences Commons
See next page for additional authors

Right click to open a feedback form in a new tab to let us know how this document benefits you.

Repository Citation

Dai, Jin; Ji, Yanli; Wang, Wei; Kim, Donghern; Fai, Leonard Yenwong; Wang, Lei; Luo, Jia; and Zhang, Zhuo, "Loss of Fructose-1,6-Bisphosphatase Induces Glycolysis and Promotes Apoptosis Resistance of Cancer Stem-Like Cells: An Important Role in Hexavalent Chromium-Induced Carcinogenesis" (2017). *Toxicology and Cancer Biology Faculty Publications*. 83.
https://uknowledge.uky.edu/toxicology_facpub/83

This Article is brought to you for free and open access by the Toxicology and Cancer Biology at UKnowledge. It has been accepted for inclusion in Toxicology and Cancer Biology Faculty Publications by an authorized administrator of UKnowledge. For more information, please contact UKnowledge@lsv.uky.edu.

Loss of Fructose-1,6-Bisphosphatase Induces Glycolysis and Promotes Apoptosis Resistance of Cancer Stem-Like Cells: An Important Role in Hexavalent Chromium-Induced Carcinogenesis

Digital Object Identifier (DOI)
https://doi.org/10.1016/j.taap.2017.06.014

Notes/Citation Information

Published in *Toxicology and Applied Pharmacology*, v. 331, p. 164-173.

© 2017 Elsevier Inc. All rights reserved.

This manuscript version is made available under the CC-BY-NC-ND 4.0 license https://creativecommons.org/licenses/by-nc-nd/4.0/.

The document available for download is the author's post-peer-review final draft of the article.

Authors

Jin Dai, Yanli Ji, Wei Wang, Donghern Kim, Leonard Yenwong Fai, Lei Wang, Jia Luo, and Zhuo Zhang

This article is available at UKnowledge: https://uknowledge.uky.edu/toxicology_facpub/83

Author Manuscript
Author Manuscript
Author Manuscript
Author Manuscript

HHS Public Access
Author manuscript
Toxicol Appl Pharmacol. Author manuscript; available in PMC 2018 September 15.

Published in final edited form as:
Toxicol Appl Pharmacol. 2017 September 15; 331: 164–173. doi:10.1016/j.taap.2017.06.014.

Loss of fructose-1,6-bisphosphatase induces glycolysis and promotes apoptosis resistance of cancer stem-like cells: an important role in hexavalent chromium-induced carcinogenesis

Jin Dai[1], **Yanli Ji**[1], **Wei Wang**[1], **Donghern Kim**[1], **Leonard Yenwong Fai**[1], **Lei Wang**[2], **Jia Luo**[3], and **Zhuo Zhang**[1]

[1]Department of Toxicology and Cancer Biology, 1095 Veterans Drive, University of Kentucky, Lexington, KY 40536

[2]Center for Research on Environmental Diseases, 1095 Veterans Drive, University of Kentucky, Lexington, KY 40536

[3]Department of Pharmacology and Nutritional Sciences, 1095 Veterans Drive, University of Kentucky, Lexington, KY 40536

Abstract

Hexavalent chromium (Cr(VI)) compounds are confirmed human carcinogens for lung cancer. Our previous studies has demonstrated that chronic exposure of human bronchial epithelial BEAS-2B cells to low dose of Cr(VI) causes malignant cell transformation. The acquisition of cancer stem cell-like properties is involved in the initiation of cancers. The present study has observed that a small population of cancer stem-like cells (BEAS-2B-Cr-CSC) exists in the Cr(VI)-transformed cells (BEAS-2B-Cr). Those BEAS-2B-Cr-CSC exhibit extremely reduced capability of generating reactive oxygen species (ROS) and apoptosis resistance. BEAS-2B-Cr-CSC are metabolic inactive as evidenced by reductions in oxygen consumption, glucose uptake, ATP production, and lactate production. Most importantly, BEAS-2B-Cr-CSC are more tumorigenic with high levels of cell self-renewal genes, Notch1 and p21. Further study has found that fructose-1,6-bisphosphatase (FBP1), an rate-limiting enzyme driving glyconeogenesis, was lost in BEAS-2B-Cr-CSC. Forced expression of FBP1 in BEAS-2B-Cr-CSC restored ROS generation, resulting in increased apoptosis, leading to inhibition of tumorigenesis. In summary, the present study suggests that loss of FBP1 is a critical event in tumorigenesis of Cr(VI)-transformed cells.

*To whom correspondence should be addressed: Zhuo Zhang, Department Toxicology and Cancer Biology, University of Kentucky, Lexington, KY 40536, USA. Tel.: (859)323-9591; Fax (859)323 1059; zhuo.zhang@uky.edu.

Conflict of Interest Statement
The authors declare no conflict of interest to report.

Publisher's Disclaimer: This is a PDF file of an unedited manuscript that has been accepted for publication. As a service to our customers we are providing this early version of the manuscript. The manuscript will undergo copyediting, typesetting, and review of the resulting proof before it is published in its final citable form. Please note that during the production process errors may be discovered which could affect the content, and all legal disclaimers that apply to the journal pertain.

Author Manuscript Author Manuscript Author Manuscript Author Manuscript

Keywords

Cr(VI); fructose-1; 6-bisphosphatase; cancer stem cells; metabolism; reactive oxygen species; tumorigenesis

Introduction

Glucose homeostasis is controlled by the catabolic glycolysis/oxidative phosphorylation (OXPHOS) and the anabolic gluconeogenesis pathway. Cancer cells prefer aerobic glycolysis which metabolizes glucose to lactate. Aerobic glycolysis, maximizing ATP production, does not require an increase in mitochondrial capacity (Fan *et al.*, 2013). The occurrence of Warburg effect indicates the activation of oncogenic signaling, resulting in promotion of glucose uptake and anabolic metabolism (Fan *et al.*, 2013). Fructose-1, 6-bisphosphatase (FBP1), a rate-limiting enzyme in gluconeogenesis, catalyzes the hydrolysis of fructose-1, 6-bisphosphate (F-1, 6-BP) to fructose 6-phosphate and inorganic phosphate. It has been reported that FBP1 is lost in gastric cancer (Liu *et al.*, 2010), hepatocellular carcinoma and colon cancer (Chen *et al.*, 2011), breast cancer (Dong *et al.*, 2013), lung cancer (Zhang *et al.*, 2016), and kidney cancer (Alderton, 2014). Loss of FBP1 is correlated with advanced tumor stage and poor prognosis (Chen *et al.*, 2011; Zhang *et al.*, 2016).

Cancer recurrence despite local and/or systemic therapy suggests the existence of a cell population with enormous capacity for self-renewal and regeneration, a biological function generally limited to normal somatic stem cells. Cancer stem cells (CSCs), referred to cancer initiating cells, are a phenotypically distinct population that possesses tumorigenic potential. Similar to cancer cells, CSCs utilize aerobic glycolysis for biosynthesis and energy requirement (Dong *et al.*, 2016). CSCs consume more reduced nicotinamide adenine dinucleotide (NADH) and ADP to produce more glycolysis intermediates than cancer cells (Wang *et al.*, 2014). In CSCs, many metabolic enzymes exhibit both catalytic and transcriptional activities to maintain the metabolic characteristics and to activate stem-like properties. Low level of FBP1 is beneficial to CSCs due to (a) inductions of superiority of glycolysis and increased glucose uptake, facilitating the production of glycolysis intermediates and the energy supply in CSCs during hypoxia and (b) inhibition of ROS generation induced by mitochondrial complex1, protecting CSCs from oxidative stress (Dong *et al.*, 2016).

Hexavalent chromium (Cr(VI)) compounds are confirmed human carcinogens by International Agency for Research on Cancer (IARC) and US Environmental Protection Agency (EPA). Chronical Cr(VI) exposure through environment or occupation is associated with lung cancer (Langard, 1990; Woodruff *et al.*, 1998). Although the mechanisms of Cr(VI) carcinogenesis is still unclear, it is believed that reactive oxygen species (ROS) play an important role (Shi and Dalal, 1989; Stohs *et al.*, 2000; Yao *et al.*, 2008; Wang *et al.*, 2011). Our previous studies have demonstrated that once the cells are malignantly transformed, the capacity of generating ROS is reduced, resulting in apoptosis resistance and tumorigenesis of those transformed cells (Kim *et al.*, 2015). Mitochondria is the main source of ROS generation. Dysfunction of mitochondria in cancer cells results in an increase in

Author Manuscript Author Manuscript Author Manuscript Author Manuscript

aerobic glycolysis (Boland *et al.*, 2013). Linkage between the perturbed metabolism and reduced capacity of ROS generation in Cr(VI)-transformed cells are unknown. Especially tumorigenic effect of CSCs remains to be investigated. It has been reported that ROS generation was reduced in the FBP1 mutant cells in response to treatment with methylmethane sulfonate, an alkylating agent (Kitanovic and Wolfl, 2006). Low ROS levels in CSCs are critical for the maintenance of self-renewal of hematopoietic stem cells and human and mouse breast CSCs (Diehn *et al.*, 2009). Inhibition of FBP1 caused delayed ROS generation, resulting in increased survival of aged cells (Kitanovic and Wolfl, 2006).

The present study investigated the self-renewal and proliferation of CSCs isolated from Cr(VI)-transformed cells and their ability for driving tumorigenesis. The present study also investigated the mechanism of apoptosis resistance of those CSCs and metabolic switch to glycolysis.

Materials and Methods

Chemicals and reagents

Sodium dichromate dehydrate ($Na_2Cr_2O_7$) was from Sigma (St Louis, MO). Cisplatin was from Enzo Life Sciences (Farmingdale, NY). Dulbecco's modified Eagle's medium (DMEM), Defined keratinocyte serum-free medium, fetal bovine serum (FBS), and Oligo $(dT)_{20}$ and AccuPrime Taq DNA Polymerase High Fidelity were from Invitrogen (Carlsbad, CA). Bradford Protein Assay Reagent was from Bio-Rad (Hercules, CA). RNeasy Mini kit and plasmid prep kit were from Qiagen (Valencia, CA). M-MLV reverse transcriptase was from Promega (Madison, WI). Perfecta Sybr Green Fastmix was from Quanta Biosciences (Gaithersburgh, MD). 5-(and -6)-chloromethyl-2, 7-dichlorodihydrofluorescein diacetate, acetyl ester (CM-H_2DCFDA) and CellROX deep red reagent were from Molecular Probes (Eugene, OR). Antibodies against NQO1, GAPDH, and β-actin were obtained from Santa Cruz (Santa Cruz, CA). Antibody against FBP1 was from Sigma (St Louis, MO). Antibody against SOD2 was from Millipore (Billerica, MA). Antibodies against Notch1, p21, cyclin D1, Bcl-2, Bcl-xL, PARP, AP1/c-jun, cleaved caspase 3, and cleaved caspase 9 were from Cell Signaling Tech (Danvers, MA). Enhanced chemiluminescence reagent was from Amersham (Pittsburgh, PA). Matrigel was from BD Biosciences (San Jose, CA).

Cell culture and treatment

The human bronchial epithelial cell line BEAS-2B was obtained from the American Type Culture Collection (Rockville, MD). Cells were maintained in DMEM supplemented with 10% heat-inactivated FBS and 1% penicillin–streptomycin at 37°C, 5% CO_2. The cells were exposed continuously to $Na_2Cr_2O_7$ (100 nM) in the media for 3 months and transformed cells were obtained by soft agar colony formation assay as described previously (Son *et al.*, 2013). A single colony from soft agar was picked up and continued to growth. These cells are considered as Cr(VI)-transformed cells.

Isolation and expansion of spheroid-derived cells from Cr(VI)-transformed BEAS-2B cells

The transformed BEAS-2B cells (1×10^6 cells) were re-suspended in serum-free medium with Matrigel basement membrane matrix (BD Biosciences) at a 1:1 ratio (total volume =

Author Manuscript Author Manuscript Author Manuscript Author Manuscript

100 μL) and subcutaneously injected into the flanks of nude mice. After diameter of the tumor reached about 1.5 cm, the animals were euthanized using CO_2. Tumors were isolated and cut it into small pieces followed by digestion using collagenase to prepare single cell suspension. The collected single cells were cultured in monolayer at 37°C, 5% CO_2 in DMEM supplemented with 10% heat-inactivated FBS and 1% penicillin–streptomycin. Those Cr(VI)-transformed BEAS-2B cells (BEAS-2B-Cr) were used as a pool for selection of cancer stem cells. Briefly, after BEAS-2B-Cr were grown to 100% confluence, free-floating cells were collected and cultured in defined keratinocyte serum-free medium in ultra-low attachment plates. After 6 days, spheroids formed by floating cells were collected and the cells were subcultured every 6 days. After 10 passages, those spheroid-derived cells which consistently formed spheres are considered as cancer stem cells (BEAS2B-Cr-CSC) and were used for experiments. The images of cell morphology were captured using Olympus IX73 microscope and cell size (area, μm^2) was calculated using Olympus cellSens software.

Clonal assay

The clonal assay was performed as described previously (Plaisant *et al.*, 2011). Both BEAS-2B-Cr and BEAS-2B-Cr-CSC were plated in 6-well plates at a density of 600 cells/well and incubated for 7 days. The cells were fixed with 2% formalin for 10 min and stained with 0.5% crystal violet for 5 min. The images were captured using an Olympus IX73 microscope.

Immunoblotting analysis

The cells were grown in 10-cm cell culture dishes. The cells were harvested and cell lysates were prepared in RIPA buffer. The protein concentration was measured using Bradford protein assay reagent. 20 μg of total protein from cell lysate was separated by SDS-PAGE flowered by incubation with primary antibody. The blots were then re-probed with second antibody conjugated to horseradish peroxidase. Proteins were visualized using an enhanced chemiluminescence kit.

Apoptosis Analysis

Annexin V/propidium iodide (PI) double staining was used to measure percentile of apoptosis according to manufacturer's protocol. Briefly, the cells were seeded at 5×10^5 cells/well in 6-well plates and treated with various concentrations of Cr(VI) or cisplatin for 24 hours. The cells were washed with PBS and digested with 0.25% trypsin/EDTA followed by re-suspension in 500 μL of 1xbinding buffer and addition of Annexin V/PI. The apoptotic cells were measured using flow cytometry.

Detection of ROS

The cells were cultured in 96-well plates with 5×10^4 cells/well. The cells were treated with various concentrations of Cr(VI) or cisplatin for 24 hours and then incubated with 25 μM of H_2DCFDA for 30 min at 37°C. The cells were washed twice with PBS. Fluorescence intensity was measured using a Gemini XPS fluorescence microplate spectrofluorometer (Molecular Devices). For FBP1 or vector-expressed cells, CellROX deep red reagent was

Author Manuscript Author Manuscript Author Manuscript Author Manuscript

used as ROS detection probe and ROS level was measured using flow cytometry according to manufacturer's protocol.

Measurement of glucose uptake

The cells were seeded at 5×10^5 cells/well in 6-well plates. Cells were starved in glucose- and serum-free media for 2 hours. The cells were then subsequently incubated with 100 μM of 2-deoxyglucose (2-DG) for 2 hours. After washing with PBS, cells were collected and glucose uptake (intracellular 2-DG level) was measured using a glucose uptake colorimetric assay kit (BioVision, Milpitas, CA) according to manufacturer's protocol.

Measurement of lactate production

The cells were seeded at 1×10^5 cells/well in 24-well plates. Culture media was replaced with 500 μL of fresh culture media and incubated for 24 hours. 400 μL of supernatant media was collected from the culture and the amount of lactate production was measured using a lactate colorimetric assay kit (BioVision, Milpitas, CA) according to manufacturer's protocol.

Measurement of ATP content

To determine the intracellular ATP content, 1×10^6 cells were harvested and intracellular ATP concentration was measured using ATP assay kit (BioVision, Milpitas, CA) according to manufacturer's protocol.

Mitochondrial member potential

Mitochondrial membrane potential ($\Delta\psi_m$) was assessed using a JC-1 mitochondrial membrane potential assay kit (Cayman Chemical, Ann Arbor, MI) according to manufacturer's protocol. Briefly, the cells were incubated with a JC-1 staining solution (1:10 dilution) for 20 mins and washed with assay buffer twice. Then the fluorescence was detected using a Gemini XPS fluorescence microplate spectrofluorometer (Molecular Devices) at 488 nm excitation and 520 nm emission for green and 540 nm excitation and 590 nm emission for red. The ratio of red/green uorescence was calculated.

Detection of oxygen consumption and glycolysis

Cellular oxygen consumption and glycolysis were assessed with a mitochondria stress test and a glycolysis stress test using a Seahorse XF-96 Flux Analyzer (Agilent Technologies, Santa Clara, CA), respectively. Cells were seeded in microplates with 90% confluence and grown for overnight. For mitochondria stress test, the cell growth media was replaced with 175 uL of FX media (FX Assay Modified DMEM from Agilent Technologies with 5.5 mM glucose, 1 mM pyruvate and 2 mM glutamix) prior to the assay. Cells were washed once, media exchange was completed and then cells were equilibrated for 60 mins at 37°C in non-CO_2 incubator. Oxygen consumption rate (OCR) was measured four times and plotted as a function of cells under the basal condition followed by the sequential addition of three mitochondrial inhibitors: oligomycin A (1 mM), an ATP synthase inhibitor; carbonilcyanide p-triflouromethoxyphenylhydrazone (FCCP) (1 mM), an uncoupling agent; and a mixture of 1 mM rotenone and 1 mM antimycin A, inhibitors for mitochondrial respiratory chain complex I and III to shut down the mitochondria oxygen consumption, respectively. To

Author Manuscript Author Manuscript Author Manuscript Author Manuscript

allow comparison between cells, data are normalized and presented as OCR in pmoles/min/10^6 cells. For glycolysis stress test, non-glycolytic acidification was obtained in the absence of extracellular glucose and pyruvate. Next, cells were exposed to three compounds, with measurements of extracellular acidification rate (ECAR) after each injection. The first injection, a saturating concentration of glucose (10 mM), causes an increase in ECAR and defines the rate of glycolysis under basal conditions. The second injection, oligomycin (1 μM), inhibits mitochondrial respiration and shifts energy production toward glycolysis, revealing the maximum glycolytic capacity of the cells. The final injection, 2-deoxy-D-glucose (2-DG) (100 mM), inhibits glycolysis. The difference between maximum glycolytic capacity and glycolysis defines the glycolytic reserve. Data are normalized and presented as ECAR in mpH/min/10^6 cells.

Establishment of BEAS-2B-Cr-CSC with stably expressing FBP1

pLenti6.3/FBP1 was kindly provided by Dr. Binhua P. Zhou at the University of Kentucky. BEAS-2B-Cr-CSC were transfected with 4 μg plasmid using Lipofectamine 2000. The cells were selected using 2 μg/mL blasticidin for 1 month followed by immunoblotting analysis to verify FBP1 expression.

Real time PCR

RNA was extracted and purified using Qiagen RNeasy mini kit. 0.5 μg of RNA was reversely transcribed using M-MLV reverse transcriptase. Primers were designed using Primer-Blast yielding. Primers for human FBP1 are followed: Forward-CCC CAG ATA ATT CAG CTC CTT A and Reverse-GTT GCA TTC GTA CAG CAG TCT C. Values were normalized by GAPDH. Primers for GAPDH are followed: Forward-GCG AGA TCC CTC CAA AAT CAA and Reverse-GTT CAC ACC CAT GAC GAA CAT. PCR was performed using Perfecta Sybr Green Fastmix (Quanta Biosciences) in the CFX96 real-time PCR Detection System (Bio-Rad). Data were analyzed using CFX Manager software (Bio-Rad).

Tumorigenesis assay

Athymic nude mice (NU/NU, 6–8 weeks old, female) were purchased from The Jackson Laboratory (Bar Harbor, ME). The animals were housed in a pathogen-free room in the animal facilities at the Chandler Medical Center, University of Kentucky. All animals were handled according to the Institutional Animal Care and Use (IACUC) guidelines, University of Kentucky. The animals were randomly divided into the various groups with six animals of each group. Normal BEAS-2B cells, BEAS-2B-Cr, and BEAS-2B-Cr-CSC with or without forced expression of FBP1 were resuspended in serum-free medium with Matrigel basement membrane matrix (BD Biosciences) at a 1:1 ratio (total volume = 100 μL) and subcutaneously injected into the flanks of nude mice. Xenograft formation was examined every week up to 120 days. Tumors were measured using an external caliper and volume was calculated using the formula: (length x width^2)/2. Tumor tissues were isolated and weighed. Freshly frozen and formalin fixed tumor tissues were used for immunoblotting and immunohistochemical staining, respectively. The implantation site containing a Matrigel plug, subcutaneous tissue, peritoneum, and skin was isolated to use as control tissue corresponding to the tumor tissues.

Author Manuscript Author Manuscript Author Manuscript Author Manuscript

Statistical analysis

Data were expressed as the mean ± standard deviation (SD). Fisher's Exact Test was used to compare tumor incidence in tumorigenicity assay. In other assays, statistical significance of differences among treatment groups was determined by ANOVA with Student's t test. A $p < 0.05$ was considered as statistical significance.

Results

Isolation and characterization of spheroid-derived cells from Cr(VI)-transformed BEAS-2B cells

Our previous study has found that chronic exposure of human bronchial epithelial BEAS-2B cells to Cr(VI) causes malignant cell transformation and that those transformed cells are tumorigenic (Wang *et al.*, 2011). Cancer stem cells exhibit stem cell-like properties and have been implicated in the tumorigenesis. To test whether a rare but constant fraction of cancer stem cells is present in Cr(VI)-transformed BEAS-2B cells (BEAS-2B-Cr), free-floating cells from confluent BEAS-2B-Cr were harvested and cultured in serum-free media under anchorage-independent growth condition. Spheroids with diameter ≥50 μm were formed within 7 days. Single cells harvested from enzymatically dissociated spheroids formed second spheroids under the same culture conditions. Those spheroid cells are considered as cancer stem cells (BEAS-2B-Cr-CSC). This procedure has been repeated for over 60 passages with extensive amplification of cells. The morphology of BEAS-2B-Cr and BEAS-2B-Cr-CSC are shown in Fig. 1A. The average size of BEAS-2B-Cr-CSC was 4.5 times smaller than that of BEAS-2B-Cr (data not shown). BEAS-2B-Cr-CSC exclusively formed holoclones with tightly packed smaller cells, whereas BEAS-2B-Cr formed meroclones with loosely packed larger cells (Fig. 1B). The average cell number in the BEAS-2B-Cr-CSC clones is 5.7 times less than that in the BEAS-2B-Cr ones after 7 days of culture (data not shown). Self-renewal genes Notch1 and p21 were highly expressed in both BEAS-2B-Cr and BEAS-2B-Cr-CSC compared to those in passage-matched normal cells (Fig. 1C). The expression levels of those two genes are much higher in BEAS-2B-Cr-CSC than those in BEAS-2B-Cr (Fig. 1C). Protein level of activator protein 1 (AP1) was increased in the BEAS-2B-Cr but it was deceased in BEAS2B-Cr-CSC (Fig. 1C). The above results suggest that a small population of cancer stem cells exist in Cr(VI)-transformed cells and those cancer stem cells possess a high self-renewal but a low proliferative potential.

The gold standard to evaluate activity of cancer stem cells is their capability to initiate serially transplantable tumor development (Tang *et al.*, 2007). To determine tumor-initiating capacity of BEAS-2B-Cr-CSC, immunocompromised nude mice were injected with different cell number ranging from 1,000 to 500,000 cells. The results show that both BEAS-2B-Cr and BEAS-2B-Cr-CSC initiated tumor development in the nude mice (Fig. 1D). BEAS-2B-Cr-CSC generated more tumors than BEAS-2B-Cr at cell number less than 100,000. As few as 1,000 of BEAS-2B-Cr-CSC developed tumor in 6 out of a total of 6 animals (100% tumor incidence) (Fig. 1D). The number of tumor was significantly reduced in the animals injected with 1,000 of BEAS-2B-Cr (2 out of a total of 6 animals, 33.3% tumor incidence). The results from pathohistological analysis showed that BEAS-2B-Cr-CSC lost regular elongated shape of normal epithelial cells and exhibited significant nuclear

Author Manuscript Author Manuscript Author Manuscript Author Manuscript

pleomorphism (Fig. 1E), indicating an enhanced malignancy. Those results suggest that BEAS-2B-Cr-CSC are highly tumorigenic and may be a major contributor in tumorigenesis of Cr(VI)-transformed cells.

Reduced capability to generate reactive oxygen species (ROS) and increased apoptosis resistance in BEAS-2B-Cr-CSC

Long-lived and quiescent potentials with high resistance to apoptosis are key characteristics of cancer stem cells. To evaluate whether BEAS-2B-Cr-CSC are resistant to apoptosis, passage-matched normal BEAS-2B cells, BEAS-2B-Cr, and BEAS-2B-CrSC were treated with Cr(VI) or cisplatin, a chemotherapeutical agent, and apoptosis was evaluated. The results showed the apoptosis induced by either Cr(VI) or cisplatin treatment in BEAS-2B-Cr was reduced compared to that in normal BEAS-2B cells (Fig. 2A). Treatment with 10 μM of Cr(VI) induced 47.4% and 18.7% of apoptosis in normal BEAS-2B cells and BEAS-2B-Cr, respectively, but it was unable to induce apoptosis (0.825%) in BEAS-2B-Cr-CSC (Fig. 2A, left). Similar results were observed when those cells were treated with cisplatin (Fig. 2A, right). Those results indicate that BEAS-2B-Cr-CSC are highly resistant to apoptosis. Further study showed levels of anti-apoptotic proteins Bcl-2 and Bcl-xL were dramatically elevated in both BEAS-2B-Cr and BEAS-2B-Cr-CSC compared to passage-matched normal cells and their expressions were much higher in BEAS-2B-Cr-CSC than those in BEAS-2B-Cr (Fig. 2B).

Our previous study has demonstrated that ROS play a major role in Cr(VI)-induced cell transformation (Wang *et al.*, 2011). Our previous study has also demonstrated that at early stage of Cr(VI)-induced carcinogenesis (cell transformation), excess amount of ROS is oncogenic and at late stage of Cr(VI)-carcinogenesis (progress of transformed cells to tumors), decreased level of ROS is carcinogenic (Kim *et al.*, 2015). To explore the mechanism of apoptosis resistance in BEAS-2B-Cr-CSC, the cells were treated with Cr(VI) or cisplatin and ROS generation was measured. The results showed that basal ROS levels (without any treatment) in BEAS-2B-Cr and BEAS-2B-Cr-CSC were 0.43- and 0.31-fold of that in normal BEAS-2B cells, respectively (Fig. 2C). 10 μM of Cr(VI) treatment in normal cells induced a 8-fold increase in ROS generation compared to that without Cr(VI) treatment. It was 5-fold and 0.81-fold in BEAS-2B-Cr and BEAS-2B-Cr-CSC (Fig. 2C, left), respectively. These results indicate that extremely low capability to generate ROS may contribute to apoptosis resistance of BEAS-2B-Cr-CSC.

Because one of the major endogenous sources of ROS in eukaryotic cells is respiration in mitochondria, we examined oxygen consumption rate (OCR). As shown in Fig. 2D, basal OCR in both BEAS-2B-Cr and BEAS-2B-CSC were lower than that in passage-matched normal cells and the lowest basal OCR was found in BEAS-2B-Cr-CSC. Similar results were observed in ATP-linked and maximal OCR (Fig. 2D). Intracellular ROS level is controlled by endogenous ROS scavenging systems such as superoxide dismutase (SOD), NAD(P)H quinine oxidoreductase (NQO1). Our results showed that levels of both mitochondrial SOD (SOD2) and NQO1 were dramatically increased in BEAS-2B-Cr compared to those in the passage-matched normal ones and that the levels of those two enzymes were much higher in BEAS-2B-Cr-CSC (Fig. 2E). Altogether, these results reveal

Author Manuscript Author Manuscript Author Manuscript Author Manuscript

that elevated levels of antioxidants and reduced ROS generation cause development of apoptosis resistance in BEAS-2B-Cr-CSC.

Elevation of glycolysis and loss of FBP1 in BEAS-2B-Cr-CSC

Reduced oxygen consumption may implicate aberrant energy metabolism, we further investigated glucose metabolism in BEAS-2B-Cr-CSC. The results showed that glucose uptake, lactate production, and intracellular ATP content in BEAS-2B-Cr-CSC were 17% (Fig. 3A), 43% (Fig. 3B), and 59% (Fig. 3C) of those in BEAS-2B-Cr, respectively, indicating that BEAS-2B-Cr-CSC are metabolically inactive. Compared to passage-matched normal cells, BEAS-2B-Cr exhibit an elevation of lactate production (Fig. 3B), suggesting a metabolic shift to glycolysis. Glucose uptake in BEAS-2B-Cr was increased (Fig. 3A) and ATP content was decreased by 9% as compared to those in normal BEAS-2B cells (Fig. 3C), which may due to the reduction in oxidative phosphorylation implicated by reduced OCR as shown in Fig. 2D. Mitochondrial potential ($\Delta\psi_m$) remained the similar in BEAS-2B-Cr compared to that in passage-matched normal cells, but it was remarkably increased in BEAS-2B-Cr-CSC (Fig. 3D). It has been reported that expression of FBP1, a rate-limiting enzyme in gluconeogenesis, is reduced in many types of cancers including kidney cancer, liver cancer, colon cancer, and gastric cancer (Chen *et al.*, 2011; Alderton, 2014). As shown in Fig. 3, FBP1 expression was reduced in BEAS-2B-Cr and was depleted in BEAS-2B-Cr-CSC at both translational (Fig. 3D) and transcriptional level (Fig. 3E). Results from immunostaining analysis confirmed that FBP1 was lost in xenograft tumors generated by injection of BEAS-2B-Cr-CSC to animals (Fig. 3F).

FBP1 suppresses glycolysis and induces ROS generation, resulting in restored apoptosis in BEAS-2B-Cr-CSC

To investigate the role of FBP1 in maintaining cancer stem cell properties of BEAS-2B-Cr-CSC, stable expression of FBP1 was established (Fig. 4A). Forced expression of FBP1 reduced both glucose uptake and lactate production (Figs. 4B and 4C), indicating that FBP1 antagonizes glycolysis. The results from ECAR analysis showed that forced expression of FBP1 decreased glycolysis and glycolytic capacity, but not glycolytic reserved capacity (Fig. 4D). However, forced expression of FBP1 was unable to restore the oxygen consumption in BEAS-2B-Cr-CSC (4E). Basal, maximal, and ATP-linked OCR were all reduced by ectopic FBP1 (Fig. 4E). Those results indicates the inhibition on oxidative phosphorylation and reduction of oxygen consumption in BEAS-2B-Cr-CSC.

Forced FBP1 expression increased ROS generation and apoptosis induced by Cr(VI) and cisplatin in BEAS-2B-Cr-CSC (Figs. 5A and 5B). Expressions of anti-apoptotic proteins Bcl-2 and Bcl-xL were reduced in BEAS-2B-Cr-CSC with FBP1 overexpression compared with scramble cells (Fig. 5C). Cr(VI) treatment increased levels of cleaved PARP (C-PARP), cleaved caspase-3 (C-caspase 3), and cleaved caspase-9 (C-caspase 9) in BEAS-2B-Cr-CSC (Fig. 5C). Forced FBP1 expression reduced expressions of apoptotic proteins Bcl-2 and Bcl-xL in BEAS-2B-Cr-CSC compared to those in scramble cells (Fig. 5C). In addition, SOD2 level was also reduced in BEAS-2B-Cr-CSC with forced FBP1 expression (Fig. 5C). Those results indicate that FBP1 restores capability of generating ROS in BEAS-2B-Cr-CSC and reduces antioxidants level, leading to increased apoptosis.

Author Manuscript Author Manuscript Author Manuscript Author Manuscript

FBP1 suppresses tumorigenesis of BEAS-2B-Cr-CSC

We note that Notch1 and p21, two cell self-renewal genes, were upregulated in BEAS-2B-Cr-CSC (Fig. 1C). Next, we investigated whether FBP1 plays a role in upregulations of Notch1 and p21 in BEAS-2B-Cr-CSC. The results from immunoblotting analysis showed that both Notch 1 and p21 expressions were decreased in BEAS-2B-Cr-CSC with forced FBP1 expression compared to those in scramble cells (Fig. 6A). In contrast, forced expression of FBP1 was able to partially restore AP1 expression which was dramatically reduced in BEAS-2B-CSC cells (Fig. 6A). To further study the role of FBP1 in tumorigenesis of BEAS-2B-Cr-CSC in vivo, 1,000 of BEAS-2B-Cr-CSC with or without forced FBP1 expression were subcutaneously injected into the immunocompromised nude mice. The results show that 4 out of a total of 6 animals (66.7%) injected with FBP1-expressed BEAS-2B-Cr-CSC developed tumor after 120 days whereas 6 out of 6 (100%) injected with scramble BEAS-2B-Cr-CSC developed tumor (Fig. 6B). Both tumor weight and volume were significantly reduced in FBP1-expressed BEAS-2B-Cr-CSC compared to the scramble cells (Figs. 6B and 6C). Expressions of Notch1 and p21 were both reduced in the tumor tissue injected with BEAS-2B-Cr-CSC with forced FBP1 expression (Figs. 6D and 6E). AP1 level was elevated in the tumor tissues injected with FBP1 expressing cells (Figs. 6D and 6E). Those results suggest that FBP1 decreases expressions of Notch1 and p21, elevates level of AP1, and suppresses tumorigenesis of BEAS-2B-Cr-CSC.

Discussion

Cancer cells are derived hierarchically from a small subset of malignant cells that have a high capacity of self-renewal and differentiation—referred to cancer stem cells (CSCs) or cancer-initiating cells. CSCs exhibit stem cell-like properties and have been implicated in the tumorigenesis of basal like breast cancer, a particularly aggressive, metastatic and chemotherapy-resistant type of breast cancer (Schieber and Chandel, 2013). In the present study, we have observed that a minor fraction (about 1%) of the cells established a holoclone in Cr(VI)-transformed cells. A holoclone, a tightly packed clone, contains stem cells and progenitors (Locke *et al.*, 2005). These holoclones can be subcloned and propagated, indicating the presence of self-renewing cells in the clones (Tang *et al.*, 2007). Such a smaller fraction of cells survived and formed a sphere in anchorage independent assay, confirming existing of cancer stem-like cells in Cr(VI)-transformed cells. CSCs exhibit an enhanced capacity to initiate and sustain tumor growth, which is crucial for the progression and relapse of malignant tumors (Visvader and Lindeman, 2008). The present study has demonstrated that those CSCs are tumorigenic as evidenced development of tumor in the nude mice injected with as few as 1,000 cells.

Notch signaling is an important regulator in balance between self-renewal and differentiation in normal stem cells. How CSCs are maintained in a heterogeneous tumor is unknown. One potential contributor is the Notch signaling. It has been reported that inhibition of Notch signaling led to a decrease in CSCs number and impairs CSCs function (Abel *et al.*, 2014). It has also been reported that p21, a cell cycle inhibitor, is critical in maintaining self-renewal of leukemia stem cells (Viale *et al.*, 2009). Activation of p21 imposes cell cycle restriction and triggers repair of the damaged DNA, resulting in initiation and maintenance of leukemia

Author Manuscript Author Manuscript Author Manuscript Author Manuscript

(Viale *et al.*, 2009). The present study has shown that expressions of both Notch1 and p21 are elevated in Cr(VI)-transformed cells compared to those in passage-match normal cells. Their expressions are even higher in BEAS-2B-Cr-CSC than those in Cr(VI)-transformed cells, indicating the high capacity of self-renewal and differentiation of BEAS-2B-Cr-CSC. AP1, a transcript factor, is a homodimer or heterodimer composed of c-Jun and c-Fos families. AP1 is involved in multiple cellular processes, such as differentiation, proliferation, and apoptosis (Ameyar *et al.*, 2003; Hess *et al.*, 2004). It has been reported that activation of c-Jun facilitates entry of the cells into G1 and S phases of cell cycle (Bakiri *et al.*, 2000). c-Jun also controls anti-proliferative cell cycle regulators such as p53 (Weitzman *et al.*, 2000) and p21 (Shaulian and Karin, 2001). The results from the present study showed that protein level of AP1 was elevated in the Cr(VI)-transformed cells, but it was reduced in BEAS-2B-CSC. It has also reported that suppression of either c-Fos or c-Jun increases expressions of stemness transcription factors NANOG and SOX2 in colorectal cancer cells (Apostolou *et al.*, 2013). Elevation of AP1 in Cr(VI)-transformed cells may promote cell growth and proliferation. Reduction of AP1 in BEAS-2B-Cr-CSC causes the cell cycle restriction, maintaining stemness.

CSCs contain lower ROS levels than their corresponding non-tumorigenic cells (Diehn *et al.*, 2009; Ye *et al.*, 2011). Low levels of ROS, which are thought to be the byproducts of mitochondrial biogenesis, are required for haemopoietic stem cells (HSCs) to remain quiescent and retain their stem features, such as self-renewal potential and multipotency (Chen *et al.*, 2009). The low levels of ROS in CSCs are associated with elevated expressions of free radical scavenging systems (Zhou *et al.*, 2003; Diehn *et al.*, 2009). The strong antioxidant defense helps in the maintenance of stemness and tumourigenic capacities of CSCs, causing therapy resistance (Diehn *et al.*, 2009; Pasto *et al.*, 2014). The present study has observed that the BEAS-2B-Cr-CSC were resistant to apoptosis irritated by Cr(VI) and by cisplatin and that capacity of generating ROS in BEAS-2B-Cr-CSC were dramatically reduced. It should be noted that reduced capacity of generating ROS is one of the major players for apoptosis resistance of BEAS-2B-Cr-CSC. Further study has found that levels of antioxidant enzymes SOD2 and NQO1 are upregulated in BEAS-2B-Cr-CSC. Nuclear factor erythroid-related factor 2 (Nrf2), a transcription factor, is a master regulator of intercellular ROS. Nrf2 mediates the expression of cytoprotective genes, including glutathione, thioredoxin, heme oxygenase-1, NQO1, and the members of the glutathione-S-transferase family. Constitutive expression of Nrf2 is prominent in several types of human cancer cell lines and tumors (Tong *et al.*, 2006; Ohta *et al.*, 2008; Lau *et al.*, 2013). Nrf2 may help in maintaining the quiescence of hematopoietic stem cells by maintaining a reduced redox state (Shi *et al.*, 2012). Our preliminary study has observed that Nrf2 is constitutively activated in BEAS-2B-Cr-CSC. Constitutive activation of Nrf2 further causes the upregulation of its downstream cytoprotective proteins SOD2 and NQO1, resulting in reduced generation of ROS, leading to development of apoptosis resistance. Constitutively activated Nrf2 binds to AREs of Bcl-2 and Bcl-xL gene promoters, leading to up-regulations of antiapoptotic Bcl-2 and Bcl-XL and development of resistance to apoptosis (Calvert *et al.*, 2009; Niture and Jaiswal, 2012; Son *et al.*, 2015). Our unpublished results have shown that binding of Nrf2 to AREs in the promoters of Bcl-2, Bcl-xL, SOD2, and NOQ1 in Cr(VI)-transformed cells

Author Manuscript Author Manuscript Author Manuscript Author Manuscript

were markedly increased. We anticipate that the similar observations will be obtained in BEAS-2B-Cr-CSC as those in BEAS-2B-Cr.

Metabolic adaptation is one of the hallmarks of cancer cells. Glycolysis is the enzymatic conversion of glucose into lactate, which produces 2 molecules of ATP per molecule of glucose. In the presence of oxygen, cells adopt oxidative phosphorylation as a major pathway to produce energy, more efficiency than glycolysis since it generates 36 molecules of ATP per molecule of glucose. Cancer cells generate ATP via glycolysis even under normoxic concentrations known as the Warburg effect (Peiris-Pages *et al.*, 2016). Glycolysis produces ATP more rapidly than OXPHOS in the presence of abundant glucose (Guppy *et al.*, 1993). Compared to the passage-matched normal BEAS-2B cells, Cr(VI)-transformed cells generated more lactate without significant changes in glucose uptake and ATP production, indicating a switch from mitochondrial respiration to a metabolism that is mainly glycolytic.

It has been reported that CSCs are less glycolytic, consume less glucose, produce less lactate, and maintain higher ATP levels than their differentiated progeny. However, other studies have reported that CSCs are more glycolytic than their differentiated cancer cells, glucose uptake, expression of glycolytic enzymes, lactate production, and ATP content are all significantly increased (Ciavardelli *et al.*, 2014; Palorini *et al.*, 2014). This glycolytic phenotype is associated with a decrease in mitochondrial oxidative metabolism (Zhou *et al.*, 2011). In the present study we have shown that glucose uptake, lactate production, and ATP content were all remarkably reduced in BEAS-2B-Cr-CSC compared to normal cells and Cr(VI)-transformed cells, indicating metabolic inactiveness of those CSCs. The mitochondria of CSCs have an increased mass and membrane potential, which reflects mitochondrial function, higher mitochondrial ROS and enhanced oxygen consumption rates compared with the differentiated cancer cells (Lagadinou *et al.*, 2013; Pasto *et al.*, 2014; De Luca *et al.*, 2015; Lamb *et al.*, 2015; Sancho *et al.*, 2015). Another study has reported the lower quantity of mitochondrial DNA, higher mitochondrial potential, lower oxygen/glucose consumption, and lower intracellular levels of ROS and ATP content in CSCs isolated from adenocarcinomic human alveolar basal epithelial A549 cells (Ye *et al.*, 2011). In the present study, we have observed reduced levels of both mitochondrial and non-mitochondrial OCR in BEAS-2B-Cr-CSC, further showing that those CSCs are in low energy demanding. A higher $\Delta\psi_m$ is an indicator of transformation, differentiation status, and tumorigenicity. Although the present study has not detected the mitochondrial mass yet, our results showed a dramatic elevation of $\Delta\psi_m$ in BEAS-2B-Cr-CSC compared to those in passage-matched normal cells and in Cr(VI)-transformed cells. The mechanism of high $\Delta\psi_m$ in CSCs is unknown, one possibility is the overexpression of Bcl-2 family. It has been reported that the interaction of Bcl-2 and Bcl-xL with permeability transition pore complex (PTPC) facilitates closure and maintenance of $\Delta\psi_m$ (Sugrue and Tatton, 2001). In BEAS-2B-Cr-CSC, both Bcl-2 and Bcl-xL are highly expressed. High levels of Bcl-2 and Bcl-xL may explain the high $\Delta\psi_m$ of BEAS-2B-Cr-CSC. ROS, acting on thiols in the PTPC, facilitates opening of PTPC and shifts the intracellular $\Delta\psi_m$ (Klein *et al.*, 1996). The low levels of ROS may be another possibility for the high $\Delta\psi_m$ in BEAS-2B-Cr-CSC.

Author Manuscript Author Manuscript Author Manuscript Author Manuscript

FBP1 is a rate-limiting enzyme in gluconeogenesis. It has been reported that FBP1 inhibition increased glucose uptake and lactate secretion in HK-2 human renal cells (Li *et al.*, 2014). Ectopic FBP1 expression in a VHL-deficient renal carcinoma RCC10 cells reduced glucose uptake, lactate secretion, and glucose-derived TCA cycle intermediates (Li *et al.*, 2014). We manipulated FBP1 expression in BEAS-2B-Cr-CSC and measured glucose metabolism. Forced expression of FBP1 causes reductions of glucose uptake, lactate production, and glycolysis, indicating that FBP1 is a critical regulator of glucose metabolism in BEAS-2B-Cr-CSC. However, forced expression of FBP1 failed to restore the oxygen consumption. Our preliminary data showed in BEAS-2B-Cr mitochondria was defected. We speculate that chronic exposure of BEAS-2B cells to Cr(VI) causes mitochondrial damage and subsequently inhibition of mitochondrial oxidative phosphorylation in BEAS-2B-Cr and BEAS-2B-Cr-CSC, which could not be restored by ectopic expression of FBP1.

Reduced level of FBP1 is associated with tumor progression and poor prognosis (Li *et al.*, 2014; Hirata *et al.*, 2016), suggesting that FBP1 may act as tumor suppressor gene in addition to its enzymatic function. Loss of FBP1 has also been reported to inhibit ROS production, resulting in an increased CSC-like property and tumorigenicity of breast cancer cells (Dong *et al.*, 2013). Ectopic expression of FBP1 in breast cancer cells diminished tumor growth in mice (Dong *et al.*, 2013). FBP1 inhibited HIF function by direct interaction with HIF inhibitory domain, leading to suppression of proliferation of renal carcinoma cells (Li *et al.*, 2014). We have observed that forced expression of FBP1 restored the capacity of generating ROS and decreased SOD2 protein level in BEAS-2B-Cr-CSC. We have also observed that forced expression of FBP1 decreased levels of anti-apoptotic proteins Bcl-2 and Bcl-xL and elevated levels of apoptotic proteins C-PARP, C-caspase 3, and C-caspase 9 in BEAS-2B-Cr-CSC. The results from our preliminary study showed that forced expression of FBP1 in BEAS-2B-Cr-CSC decreased Nrf2 level. Reduction in Nrf2 may cause decreases of SOD2, Bcl-2, and Bcl-xL through decreased binding of Nrf2 to AREs in their promoters, resulting in increased apoptosis, leading to inhibition of tumorigenesis. Forced expression of FBP1 also decreased levels of self-renewal genes Notch1 and p21 and increased cyclin D1 level, promoting cell cycle and reducing stemness. The mechanism of FBP1 on Notch1 and p21 needs to be further investigated.

In conclusion, the present study has observed that a small population of cancer stem cells is the driving force for tumorigenecity of Cr(VI)-transformed cells. Those cells exhibit low metabolic activity, reduced ROS production, diminished FBP1 level, and increased levels of mitochondrial antioxidant SOD2 and anti-apoptotic proteins Bcl-2 and Bcl-xL. Ectopic expression of FBP1 (a) suppresses glycolysis; (b) decreases levels of SOD2; (c) restores capacity of generating ROS; (d) decreases levels of Bcl-2 and Bcl-xL; and (e) reduces levels of Notch1 and p21, diminishing stemness. FBP1 functions both as an enzyme of glycogenesis in maintenance of low glucose metabolism and as a tumor suppressor in maintenance of both low ROS level and high self-renewal, contributing to tumorigenesis of Cr(VI)-transformed cells.

Author Manuscript Author Manuscript Author Manuscript Author Manuscript

Acknowledgments

We thank Dr. Binhua P Zhou, University of Kentucky, for the gift of FBP1 overexpression construct. We also thank Dr. Xianglin Shi, University of Kentucky, for his critical comments and suggestions in the preparation of this manuscript.

Abbreviations

AP1	activator protein 1
Cr(VI)	hexavalent chromium
CSCs	cancer stem cells
2-DG	2-deoxy-D-glucose
ECAR	extracellular acidification rate
FBP1	fructose-1,6- bisphosphatase
FCCP	carbonilcyanide p-triflouromethoxyphenylhydrazone
H_2DCFDA	5-(and -6)-chloromethyl-2, 7-dichlorodihydrofluorescein diacetate, acetyl ester
NQO1	NAD(P)H dehydrogenase (quinone) 1
Nrf2	nuclear factor erythroid-related factor 2
OCR	oxygen consumption rate
OXPHOS	catabolic glycolysis/oxidative phosphorylation
PTPC	permeability transition pore complex
ROS	reactive oxygen species
SOD	superoxide dismutase
SOX2	sex determining region Y-box 2

References

Abel EV, Kim EJ, Wu J, Hynes M, Bednar F, Proctor E, Wang L, Dziubinski ML, Simeone DM. The Notch pathway is important in maintaining the cancer stem cell population in pancreatic cancer. PloS one. 2014; 9:e91983. [PubMed: 24647545]

Alderton GK. Tumorigenesis: FBP1 is suppressed in kidney tumours. Nature reviews Cancer. 2014; 14:575.

Ameyar M, Wisniewska M, Weitzman JB. A role for AP-1 in apoptosis: the case for and against. Biochimie. 2003; 85:747–752. [PubMed: 14585541]

Apostolou P, Toloudi M, Ioannou E, Chatziioannou M, Kourtidou E, Vlachou I, Papasotiriou I. AP-1 Gene Expression Levels May Be Correlated with Changes in Gene Expression of Some Stemness Factors in Colon Carcinomas. Journal of signal transduction. 2013; 2013:497383. [PubMed: 24396595]

Author Manuscript Author Manuscript Author Manuscript Author Manuscript

Bakiri L, Lallemand D, Bossy-Wetzel E, Yaniv M. Cell cycle-dependent variations in c-Jun and JunB phosphorylation: a role in the control of cyclin D1 expression. The EMBO journal. 2000; 19:2056–2068. [PubMed: 10790372]

Boland ML, Chourasia AH, Macleod KF. Mitochondrial dysfunction in cancer. Front Oncology. 2013; 3:292.

Calvert JW, Jha S, Gundewar S, Elrod JW, Ramachandran A, Pattillo CB, Kevil CG, Lefer DJ. Hydrogen sulfide mediates cardioprotection through Nrf2 signaling. Circulation research. 2009; 105:365–374. [PubMed: 19608979]

Chen C, Liu Y, Liu Y, Zheng P. The axis of mTOR-mitochondria-ROS and stemness of the hematopoietic stem cells. Cell cycle. 2009; 8:1158–1160. [PubMed: 19270502]

Chen M, Zhang J, Li N, Qian Z, Zhu M, Li Q, Zheng J, Wang X, Shi G. Promoter hypermethylation mediated downregulation of FBP1 in human hepatocellular carcinoma and colon cancer. PloS one. 2011; 6:e25564. [PubMed: 22039417]

Ciavardelli D, Rossi C, Barcaroli D, Volpe S, Consalvo A, Zucchelli M, De Cola A, Scavo E, Carollo R, D'Agostino D, Forli F, D'Aguanno S, Todaro M, Stassi G, Di Ilio C, De Laurenzi V, Urbani A. Breast cancer stem cells rely on fermentative glycolysis and are sensitive to 2-deoxyglucose treatment. Cell death & disease. 2014; 5:e1336. [PubMed: 25032859]

De Luca A, Fiorillo M, Peiris-Pages M, Ozsvari B, Smith DL, Sanchez-Alvarez R, Martinez-Outschoorn UE, Cappello AR, Pezzi V, Lisanti MP, Sotgia F. Mitochondrial biogenesis is required for the anchorage-independent survival and propagation of stem-like cancer cells. Oncotarget. 2015; 6:14777–14795. [PubMed: 26087310]

Diehn M, Cho RW, Lobo NA, Kalisky T, Dorie MJ, Kulp AN, Qian D, Lam JS, Ailles LE, Wong M, Joshua B, Kaplan MJ, Wapnir I, Dirbas FM, Somlo G, Garberoglio C, Paz B, Shen J, Lau SK, Quake SR, Brown JM, Weissman IL, Clarke MF. Association of reactive oxygen species levels and radioresistance in cancer stem cells. Nature. 2009; 458:780–783. [PubMed: 19194462]

Dong BW, Qin GM, Luo Y, Mao JS. Metabolic enzymes: key modulators of functionality in cancer stem-like cells. Oncotarget. 2016

Dong C, Yuan T, Wu Y, Wang Y, Fan TW, Miriyala S, Lin Y, Yao J, Shi J, Kang T, Lorkiewicz P, St Clair D, Hung MC, Evers BM, Zhou BP. Loss of FBP1 by Snail-mediated repression provides metabolic advantages in basal-like breast cancer. Cancer cell. 2013; 23:316–331. [PubMed: 23453623]

Fan J, Kamphorst JJ, Mathew R, Chung MK, White E, Shlomi T, Rabinowitz JD. Glutamine-driven oxidative phosphorylation is a major ATP source in transformed mammalian cells in both normoxia and hypoxia. Molecular systems biology. 2013; 9:712. [PubMed: 24301801]

Guppy M, Greiner E, Brand K. The role of the Crabtree effect and an endogenous fuel in the energy metabolism of resting and proliferating thymocytes. European journal of biochemistry. 1993; 212:95–99. [PubMed: 8444168]

Hess J, Angel P, Schorpp-Kistner M. AP-1 subunits: quarrel and harmony among siblings. Journal of cell science. 2004; 117:5965–5973. [PubMed: 15564374]

Hirata H, Sugimachi K, Komatsu H, Ueda M, Masuda T, Uchi R, Sakimura S, Nambara S, Saito T, Shinden Y, Iguchi T, Eguchi H, Ito S, Terashima K, Sakamoto K, Hirakawa M, Honda H, Mimori K. Decreased Expression of Fructose-1,6-bisphosphatase Associates with Glucose Metabolism and Tumor Progression in Hepatocellular Carcinoma. Cancer research. 2016; 76:3265–3276. [PubMed: 27197151]

Kim D, Dai J, Fai LY, Yao H, Son YO, Wang L, Pratheeshkumar P, Kondo K, Shi X, Zhang Z. Constitutive activation of epidermal growth factor receptor promotes tumorigenesis of Cr(VI)-transformed cells through decreased reactive oxygen species and apoptosis resistance development. The Journal of biological chemistry. 2015; 290:2213–2224. [PubMed: 25477514]

Kitanovic A, Wolfl S. Fructose-1,6-bisphosphatase mediates cellular responses to DNA damage and aging in Saccharomyces cerevisiae. Mutat Res. 2006; 594:135–147. [PubMed: 16199065]

Klein BY, Gal I, Libergal M, Ben-Bassat H. Opposing effects on mitochondrial membrane potential by malonate and levamisole, whose effect on cell-mediated mineralization is antagonistic. Journal of cellular biochemistry. 1996; 60:139–147. [PubMed: 8825423]

Author Manuscript Author Manuscript Author Manuscript Author Manuscript

Lagadinou ED, Sach A, Callahan K, Rossi RM, Neering SJ, Minhajuddin M, Ashton JM, Pei S, Grose V, O'Dwyer KM, Liesveld JL, Brookes PS, Becker MW, Jordan CT. BCL-2 inhibition targets oxidative phosphorylation and selectively eradicates quiescent human leukemia stem cells. Cell stem cell. 2013; 12:329–341. [PubMed: 23333149]

Lamb R, Bonuccelli G, Ozsvari B, Peiris-Pages M, Fiorillo M, Smith DL, Bevilacqua G, Mazzanti CM, McDonnell LA, Naccarato AG, Chiu M, Wynne L, Martinez-Outschoorn UE, Sotgia F, Lisanti MP. Mitochondrial mass, a new metabolic biomarker for stem-like cancer cells: Understanding WNT/FGF-driven anabolic signaling. Oncotarget. 2015; 6:30453–30471. [PubMed: 26421711]

Langard S. One hundred years of chromium and cancer: a review of epidemiological evidence and selected case reports. American journal of industrial medicine. 1990; 17:189–215. [PubMed: 2405656]

Lau A, Whitman SA, Jaramillo MC, Zhang DD. Arsenic-mediated activation of the Nrf2-Keap1 antioxidant pathway. Journal of biochemical and molecular toxicology. 2013; 27:99–105. [PubMed: 23188707]

Li B, Qiu B, Lee DS, Walton ZE, Ochocki JD, Mathew LK, Mancuso A, Gade TP, Keith B, Nissim I, Simon MC. Fructose-1,6-bisphosphatase opposes renal carcinoma progression. Nature. 2014; 513:251–255. [PubMed: 25043030]

Liu X, Wang X, Zhang J, Lam EK, Shin VY, Cheng AS, Yu J, Chan FK, Sung JJ, Jin HC. Warburg effect revisited: an epigenetic link between glycolysis and gastric carcinogenesis. Oncogene. 2010; 29:442–450. [PubMed: 19881551]

Locke M, Heywood M, Fawell S, Mackenzie IC. Retention of intrinsic stem cell hierarchies in carcinoma-derived cell lines. Cancer research. 2005; 65:8944–8950. [PubMed: 16204067]

Niture SK, Jaiswal AK. Nrf2 protein up-regulates antiapoptotic protein Bcl-2 and prevents cellular apoptosis. The Journal of biological chemistry. 2012; 287:9873–9886. [PubMed: 22275372]

Ohta T, Iijima K, Miyamoto M, Nakahara I, Tanaka H, Ohtsuji M, Suzuki T, Kobayashi A, Yokota J, Sakiyama T, Shibata T, Yamamoto M, Hirohashi S. Loss of Keap1 function activates Nrf2 and provides advantages for lung cancer cell growth. Cancer research. 2008; 68:1303–1309. [PubMed: 18316592]

Palorini R, Votta G, Balestrieri C, Monestiroli A, Olivieri S, Vento R, Chiaradonna F. Energy metabolism characterization of a novel cancer stem cell-like line 3AB-OS. Journal of cellular biochemistry. 2014; 115:368–379. [PubMed: 24030970]

Pasto A, Bellio C, Pilotto G, Ciminale V, Silic-Benussi M, Guzzo G, Rasola A, Frasson C, Nardo G, Zulato E, Nicoletto MO, Manicone M, Indraccolo S, Amadori A. Cancer stem cells from epithelial ovarian cancer patients privilege oxidative phosphorylation, and resist glucose deprivation. Oncotarget. 2014; 5:4305–4319. [PubMed: 24946808]

Peiris-Pages M, Martinez-Outschoorn UE, Pestell RG, Sotgia F, Lisanti MP. Cancer stem cell metabolism. Breast cancer research: BCR. 2016; 18:55. [PubMed: 27220421]

Plaisant M, Giorgetti-Peraldi S, Gabrielson M, Loubat A, Dani C, Peraldi P. Inhibition of hedgehog signaling decreases proliferation and clonogenicity of human mesenchymal stem cells. PloS one. 2011; 6:e16798. [PubMed: 21304817]

Sancho P, Burgos-Ramos E, Tavera A, Bou Kheir T, Jagust P, Schoenhals M, Barneda D, Sellers K, Campos-Olivas R, Grana O, Viera CR, Yuneva M, Sainz B Jr, Heeschen C. MYC/PGC-1alpha Balance Determines the Metabolic Phenotype and Plasticity of Pancreatic Cancer Stem Cells. Cell metabolism. 2015; 22:590–605. [PubMed: 26365176]

Schieber MS, Chandel NS. ROS links glucose metabolism to breast cancer stem cell and EMT phenotype. Cancer cell. 2013; 23:265–267. [PubMed: 23518342]

Shaulian E, Karin M. AP-1 in cell proliferation and survival. Oncogene. 2001; 20:2390–2400. [PubMed: 11402335]

Shi X, Zhang Y, Zheng J, Pan J. Reactive oxygen species in cancer stem cells. Antioxidants & redox signaling. 2012; 16:1215–1228. [PubMed: 22316005]

Shi XL, Dalal NS. Chromium (V) and hydroxyl radical formation during the glutathione reductase-catalyzed reduction of chromium (VI). Biochem Biophys Res Commun. 1989; 163:627–634. [PubMed: 2550002]

Author Manuscript Author Manuscript Author Manuscript Author Manuscript

Son YO, Pratheeshkumar P, Roy RV, Hitron JA, Wang L, Divya SP, Xu M, Luo J, Chen G, Zhang Z, Shi X. Antioncogenic and Oncogenic Properties of Nrf2 in Arsenic-induced Carcinogenesis. The Journal of biological chemistry. 2015; 290:27090–27100. [PubMed: 26385919]

Son YO, Pratheeshkumar P, Wang L, Wang X, Fan J, Kim DH, Lee JY, Zhang Z, Lee JC, Shi X. Reactive oxygen species mediate Cr(VI)-induced carcinogenesis through PI3K/AKT-dependent activation of GSK- 3beta/beta-catenin signaling. Toxicology and applied pharmacology. 2013; 271:239–248. [PubMed: 23707771]

Stohs SJ, Bagchi D, Hassoun E, Bagchi M. Oxidative mechanisms in the toxicity of chromium and cadmium ions. Journal of environmental pathology, toxicology and oncology: official organ of the International Society for Environmental Toxicology and Cancer. 2000; 19:201–213.

Sugrue MM, Tatton WG. Mitochondrial membrane potential in aging cells. Biological signals and receptors. 2001; 10:176–188. [PubMed: 11351127]

Tang DG, Patrawala L, Calhoun T, Bhatia B, Choy G, Schneider-Broussard R, Jeter C. Prostate cancer stem/progenitor cells: identification, characterization, and implications. Molecular carcinogenesis. 2007; 46:1–14. [PubMed: 16921491]

Tong KI, Katoh Y, Kusunoki H, Itoh K, Tanaka T, Yamamoto M. Keap1 recruits Neh2 through binding to ETGE and DLG motifs: characterization of the two-site molecular recognition model. Molecular and cellular biology. 2006; 26:2887–2900. [PubMed: 16581765]

Viale A, De Franco F, Orleth A, Cambiaghi V, Giuliani V, Bossi D, Ronchini C, Ronzoni S, Muradore I, Monestiroli S, Gobbi A, Alcalay M, Minucci S, Pelicci PG. Cell-cycle restriction limits DNA damage and maintains self-renewal of leukaemia stem cells. Nature. 2009; 457:51–56. [PubMed: 19122635]

Visvader JE, Lindeman GJ. Cancer stem cells in solid tumours: accumulating evidence and unresolved questions. Nature reviews Cancer. 2008; 8:755–768. [PubMed: 18784658]

Wang J, Christison TT, Misuno K, Lopez L, Huhmer AF, Huang Y, Hu S. Metabolomic profiling of anionic metabolites in head and neck cancer cells by capillary ion chromatography with Orbitrap mass spectrometry. Analytical chemistry. 2014; 86:5116–5124. [PubMed: 24766394]

Wang X, Son YO, Chang Q, Sun L, Hitron JA, Budhraja A, Zhang Z, Ke Z, Chen F, Luo J, Shi X. NADPH oxidase activation is required in reactive oxygen species generation and cell transformation induced by hexavalent chromium. Toxicological sciences: an official journal of the Society of Toxicology. 2011; 123:399–410. [PubMed: 21742780]

Weitzman JB, Fiette L, Matsuo K, Yaniv M. JunD protects cells from p53-dependent senescence and apoptosis. Molecular cell. 2000; 6:1109–1119. [PubMed: 11106750]

Woodruff TJ, Axelrad DA, Caldwell J, Morello-Frosch R, Rosenbaum A. Public health implications of 1990 air toxics concentrations across the United States. Environ Health Perspect. 1998; 106:245–251. [PubMed: 9518474]

Yao H, Guo L, Jiang BH, Luo J, Shi X. Oxidative stress and chromium(VI) carcinogenesis. Journal of environmental pathology, toxicology and oncology: official organ of the International Society for Environmental Toxicology and Cancer. 2008; 27:77–88.

Ye XQ, Li Q, Wang GH, Sun FF, Huang GJ, Bian XW, Yu SC, Qian GS. Mitochondrial and energy metabolism-related properties as novel indicators of lung cancer stem cells. International journal of cancer. 2011; 129:820–831. [PubMed: 21520032]

Zhang J, Wang J, Xing H, Li Q, Zhao Q, Li J. Down-regulation of FBP1 by ZEB1-mediated repression confers to growth and invasion in lung cancer cells. Molecular and cellular biochemistry. 2016; 411:331–340. [PubMed: 26546081]

Zhou Y, Hileman EO, Plunkett W, Keating MJ, Huang P. Free radical stress in chronic lymphocytic leukemia cells and its role in cellular sensitivity to ROS-generating anticancer agents. Blood. 2003; 101:4098–4104. [PubMed: 12531810]

Zhou Y, Zhou Y, Shingu T, Feng L, Chen Z, Ogasawara M, Keating MJ, Kondo S, Huang P. Metabolic alterations in highly tumorigenic glioblastoma cells: preference for hypoxia and high dependency on glycolysis. The Journal of biological chemistry. 2011; 286:32843–32853. [PubMed: 21795717]

Author Manuscript Author Manuscript Author Manuscript Author Manuscript

Highlights

- A small population of cancer-like stem cells exist in Cr(VI)-transformed cells.
- Those cancer-like stem cells are low in ROS levels and resistant to apoptosis.
- Those cancer-like stem cells are metabolic inactive and loss of FBP1.
- Those cancer-like stem cells initiate and sustain tumor growth.
- Forced expression of FBP1 inhibits tumorigenecity of those cancer-like stem cells.

Author Manuscript Author Manuscript Author Manuscript Author Manuscript

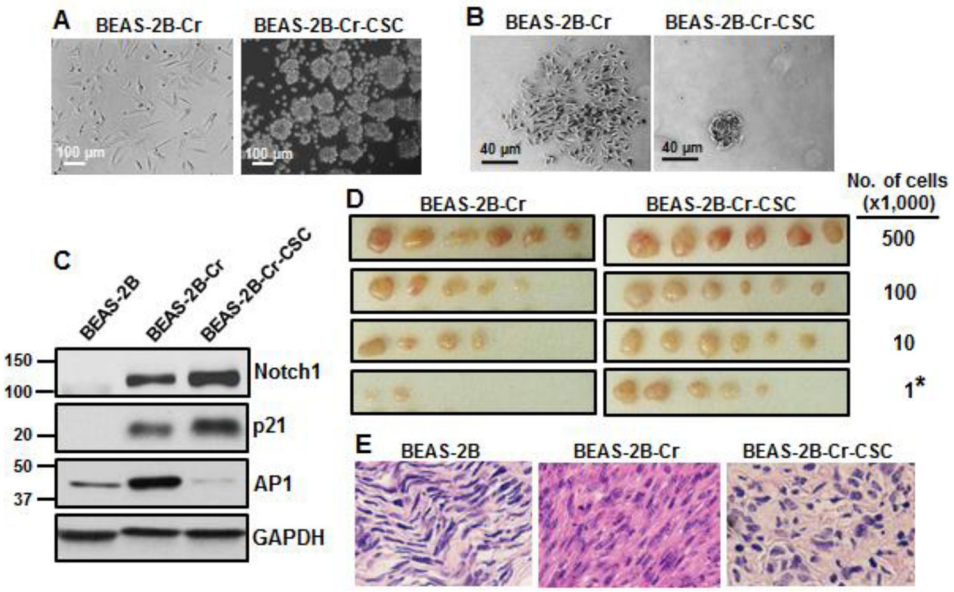

Figure 1.

Isolation and characterization of cancer-like stem cells (BEAS2B-Cr-CSC) from Cr(VI)-transformed BEAS-2B cells (BEAS-2B-Cr). (A) Representative images of BEAS-2B-Cr (monolayer) and BEAS-2B-Cr-CSC (spheroids). (B) Representative images of single clone formed by BEAS-2B-Cr (meroclone) and BEAS-2B-Cr-CSC (holoclone). (C) BEAS-2B, BEAS-2B-Cr, and BEAS-2B-Cr-CSC were harvested and whole protein lysates were isolated. Expression of Notch1, p21, and AP1 were examined using immunoblotting analysis. (D) and (E) Xenograft tumor growth. 6–8 week old, female immunocompromised nude mice were randomly divided into eight groups with six animals of each group. The animals were subcutaneously injected the various cell types and cell numbers as indicated. 90 days after implantation, the animals were euthanized and tumors were isolated. The images of tumors were captured (D). * $p<0.05$ compared to BEAS-2B-Cr group. Tumor tissues were fixed in 10% formalin. Tissue sections were subjected to hematoxylin/eosin (HE) staining (E). The results are representative of three independent experiments.

Author Manuscript Author Manuscript Author Manuscript Author Manuscript

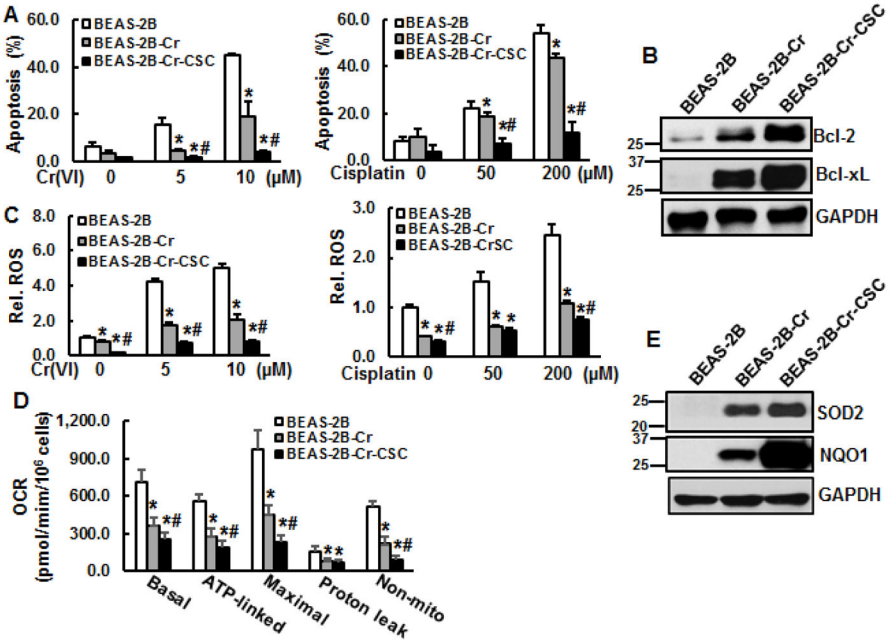

Figure 2.

Reduced ROS generation and apoptosis resistance of BEAS2B-Cr-CSC. (A) Passage-matched normal BES-2B cells, BEAS-2B-Cr, and BEAS-2B-Cr-CSC were treated with various doses of Cr(VI) or cisplatin for 24 hours. Apoptosis was determined by Annexin V/PI using flow cytometry. (B) and (E) BEAS-2B, BEAS-2B-Cr, and BEAS-2B-Cr-CSC were harvested and whole protein lysates were isolated for examination of expressions of anti-apoptotic proteins Bcl-2 and Bcl-xL (B) and antioxidant enzymes SOD2 and NQO1 (E). The results are representative of three independent experiments. (C) Intracellular ROS levels were measured by DCFDA fluorescence using a fluorescence microplate reader. Data were normalized as compared with the ROS level in BEAS-2B cells without treatment. * and #, $p<0.05$ compared to BEAS-2B and BEAS-2B-Cr, respectively. (D) BEAS-2B, BEAS-2B-Cr, and BEAS-2B-Cr-CSC were subjected to mitochondria stress assay with real time oxygen consumption rate (OCR) measurements using a Seahorse XF-96 Flux Analyzer. Data were normalized and presented as OCR in pmoles/min/10^6 cells. * and #, $p<0.05$ compared to BEAS-2B and BEAS-2B-Cr, respectively.

Author Manuscript Author Manuscript Author Manuscript Author Manuscript

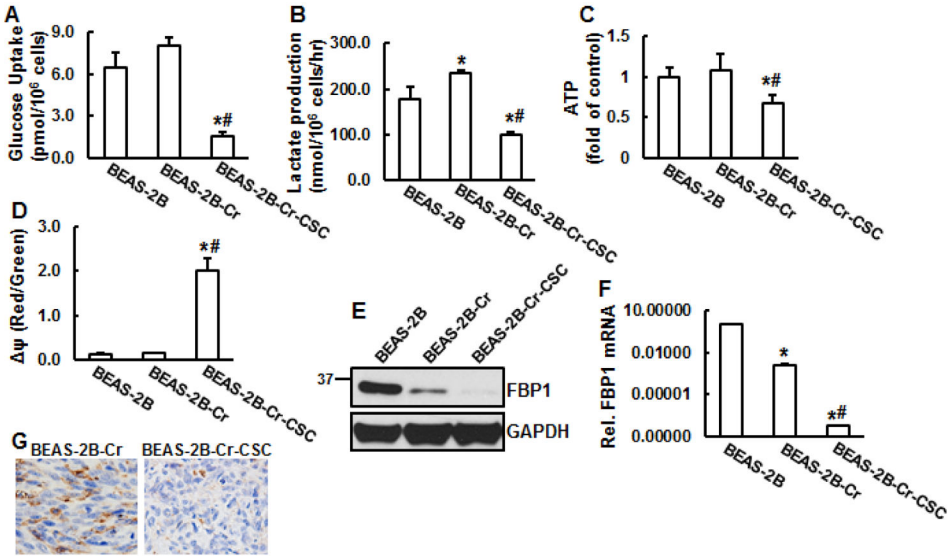

Figure 3.

Elevation of glycolysis and loss of FBP1 in BEAS-2B-Cr-CSC. Glucose uptake (A), lactate production (B), intracellular ATP contents (C), and (D) mitochondria membrane potential ($\Delta\psi_{m,}$ red/green ratio) were measured as described in the Materials and Methods. BEAS-2B cells, BEAS-2B-Cr, and BEAS-2B-Cr-CSC were harvested. Whole protein lysates (E) and mRNA (F) were isolated. Expression of FBP1 was examined using immunoblotting analysis (E) and real-time PCR (F). * and #, $p<0.05$ compared to BEAS-2B and BEAS-2B-Cr cells, respectively. (G) Representative immunohistological staining for FBP1 expression in the tumor tissues from BEAS-2B-Cr and BEAS-2B-Cr-CSC. The results are representative of three independent experiments.

Author Manuscript Author Manuscript Author Manuscript Author Manuscript

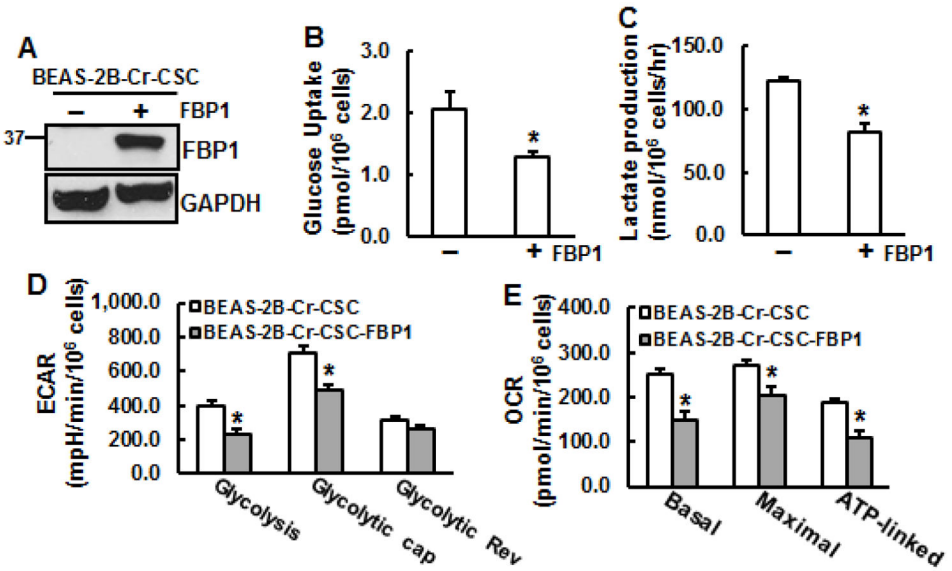

Figure 4.

FBP1 downregulates glycolysis but fails to restore oxygen consumption in BEAS-2B-Cr-CSC. (A) BEAS-2B-Cr-CSC were transfected with pLenti6.3/FBP1 followed by antibiotic selection for 1 month. The cells were harvested for examination of FBP1 expression using immunoblotting analysis. The results are representative of three independent experiments. Glucose uptake (B) and lactate production (C) in BEAS-2B-Cr-CSC with or without expression of FBP1 were measured as described in the Materials and Methods. (D) and (E) BEAS-2B-Cr-CSC with or without expression of FBP1 were subjected to glycolysis or mitochondria stress assay. Extracellular acidification rate (ECAR) (D) and oxygen consumption rate (OCR) (E) were measured using a Seahorse XF-96 Flux Analyzer. Data were normalized and presented as ECAR in mpH/min/10^6 cells and OCR in pmoles/min/10^6 cells. * $p<0.05$ compared to BEAS-2B-Cr-CSC.

Author Manuscript Author Manuscript Author Manuscript Author Manuscript

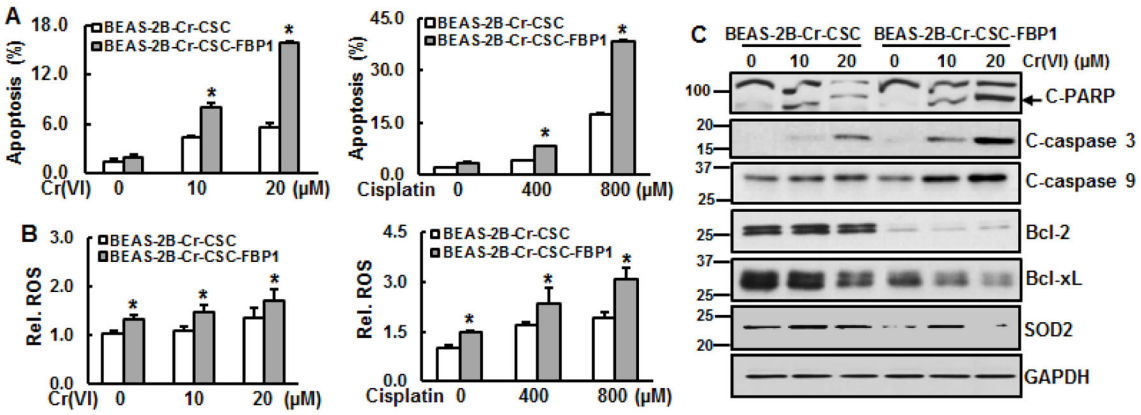

Figure 5.

FBP1 increases ROS generation and restores apoptosis of BEAS-2B-Cr-CSC. (A) and (B) BEAS-2B-Cr-CSC with or without expression of FBP1 were treated with various doses of Cr(VI) or cisplatin for 24 hours. Apoptosis was determined by Annexin V/PI using flow cytometry (A). Intracellular ROS levels were measured by CellRox deep red reagent using flow cytometry (B). Data were normalized as compared with BEAS-2B-Cr-CSC. * $p<0.05$ compared to BEAS-2B-Cr-CSC. (C) BEAS-2B-Cr-CSC with and without FBP1 overexpression were harvest and whole protein lysates were isolated. Expressions of apoptotic, anti-apoptotic, and antioxidant proteins were examined using immunoblotting. The results are representative of three independent experiments.

Author Manuscript Author Manuscript Author Manuscript Author Manuscript

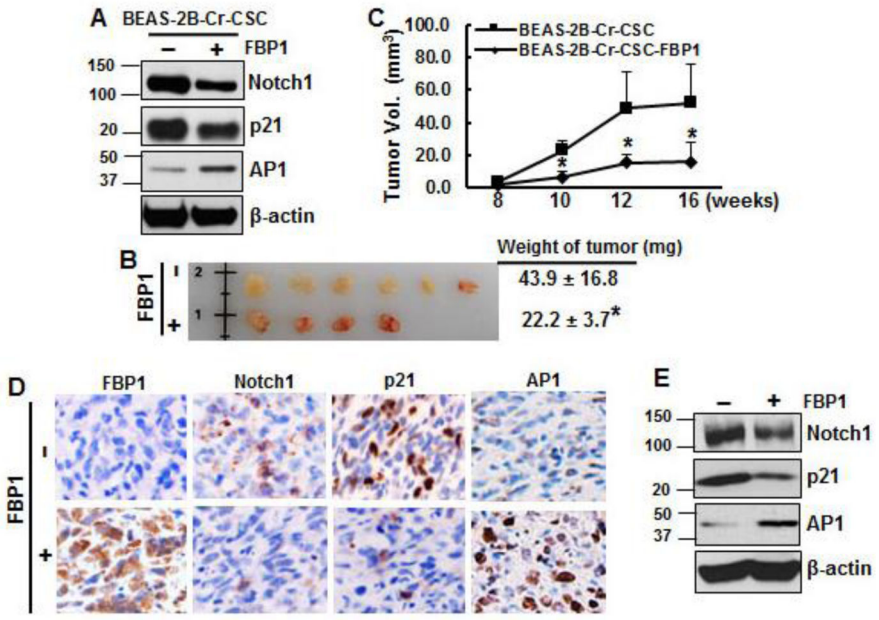

Figure 6.

FBP1 suppresses tumorigenesis of BEAS-2B-Cr-CSC. (A) BEAS-2B-Cr-CSC with and without FBP1 overexpression were collected. Whole cell lysates were isolated to examine expressions of Notch1, p21, and AP1. (B)–(E) 6–8 week old, female immunocompromised nude mice were randomly divided into two groups with six animals of each group. 1,000 of BEAS-2B-Cr-CSC with or without expression of FBP1 were subcutaneously injected in to athymic nude mice. At 120 days after implantation, animals were euthanized and xenograft tumors were isolated. Pictures were captured, tumors were weighted (B), and tumor volume were measured (C). One portion of tumor tissues was fixed in 10% formalin and another portion was freshly frozen at −80°C freezer. Tissue sections were used to examine expressions of Notch1, p21, and AP1 using immunohistological staining (D) and using immunoblotting analysis (E). The results are representative of three independent experiments.